A Study of the Products of the Reaction of Phosphorus and Dioxygen†

Charles W. Bauschlicher, Jr.*

NASA Ames Research Center, Mail Stop 230-3, Moffett Field, California 94035

Mingfei Zhou and Lester Andrews*

University of Virginia, Charlottesville, Virginia 22901

Received: October 11, 1999; In Final Form: November 30, 1999

The products of the reaction of laser-ablated red phosphorus and dioxygen have been studied using experiment and theory. The bands at 480.3 and 1273.3 cm^{-1}, previously attributed to PO_3 in the matrix isolation IR experiments, are reassigned to PO_3^-. Also observed in experiment are PO_2, PO_2^-, P_2O, OPOPO, P_4, and higher oxides.

I. Introduction

In 1988 Withnall and Andrews[1] reported the infrared (IR) spectra arising from the products of the reaction of PH_3 with atomic oxygen trapped in solid argon. They attributed bands at 480.3 and 1273.3 cm^{-1} to the a_2'' out-of-plane bend and e′ P−O stretching modes of PO_3, respectively. They also tentatively assigned a band at 435.2 cm^{-1} as the e′ bending mode of the same molecule. The assignment was based in large part on the spectra with mixed $^{16,18}O$, which clearly showed that the a_2'' mode arose from a species with three equivalent oxygen atoms, and on the fact that using PD_3, instead of PH_3, showed that the species did not include any hydrogen.

In 1989 Withnall, McCluskey, and Andrews[2] reported the electronic spectra of the species previously assigned as PO_3. They observed a band system starting at 695.5 nm with progressions of about 900 and 525 cm^{-1}. On the basis of comparison with NO_3 and SO_3^+, they assigned the observed transition as $^2E' \leftarrow X^2A_2'$, the 913 ± 10 cm^{-1} interval to the a_1' symmetric stretch in the ground state, and the 525 cm^{-1} interval to the excited state.

As part of our recent study[3] of the heats of formation of PO_n and PO_nH, $n = 1-3$, we computed the vibrational frequencies of these species. The computed frequencies of all of the molecules, except PO_3, agreed with experiment. Because we expected similar accuracy for all of the species, we looked for an alternative assignment of the experimental IR bands. We found that the computed a_2'' out-of-plane bend and the e′ stretch of PO_3^- agreed much better with the experiment than did the computed PO_3 results. Unfortunately, the computed results for neither molecule agreed well with the 435.2 cm^{-1} band.

In this paper we report on the electronic spectra and on higher level calculations for the IR spectra of PO_3 and PO_3^-. New experiments are also performed to test the PO_3^- hypotheses. Other bands are observed in these experiments, so additional calculations are performed for P_nO_m, species to aid in the identification of the observed bands. We should note that many of the P_yO_x, species have been studied by Lohr and co-workers[4] at the Hartree−Fock level. In this work, we use a higher level of theory which results in more accurate frequencies; we also consider the effect of isotopic substitution, and consider some species not considered previously.

II. Computational Methods

The geometries are optimized and the harmonic frequencies computed using the hybrid[5] B3LYP[6] functional in conjunction with the 6-31+G* and 6-31+G(2df) basis sets.[7] The vertical electronic excitation energies are computed using the time-dependent B3LYP approach[8] with the 6-31+G(d) basis set. The harmonic frequencies are also determined using the coupled cluster singles and doubles approach[9] including the effect of connected triples determined using perturbation theory,[10] CCSD-(T). All electrons are correlated in the CCSD(T) calculations. The open-shell calculations are based on unrestricted Hartree−Fock (UHF) wave functions. The 6-31G* and 6-31+G(2df) basis sets are used in conjunction with the CCSD(T) calculations.

The harmonic frequencies are computed using both ^{16}O and ^{18}O. Errors in the computed values prevent a definitive identification of the experimental bands using only the $^{16}0$ computed frequencies. However, for each band, the ratio of the frequencies determined using ^{16}O to the frequencies determined using ^{18}O, denoted R(16/18), is also computed. This ratio is more accurate than the frequencies and therefore is very helpful in identifying the bands.

The B3LYP calculations are performed using Gaussian 98,[11] while the CCSD(T) calculations are performed using ACES II.[12] The. B3LYP/6-31+G* geometries are given at http://ccf.arc.nasa.gov/~cbauschl/p2o5.geometry.

III. Experimental Methods

The experiment for laser ablation and matrix isolation has been described in detail previously.[13] Briefly, the Nd:YAG laser fundamental (1064 nm, 10 Hz repetition rate with 1−5 mJ pulses of 10 ns width) was focused on a rotating red phosphorus (Aldrich, lump) target. Laser-ablated phosphorus was codeposited with oxygen (1%) in excess argon onto a 10 K CsI cryogenic window at 2 mmol/h for l h. FTIR spectra were recorded at 0.5 cm^{-1} resolution on a Nicolet 750 spectrometer with 0.1 cm^{-1} accuracy using a HgCdTe detector. Matrix samples were annealed at different temperatures and subjected

† Part of the special issue "Marilyn Jacox Festschrift".

10.1021/jp993623b CCC: $19.00
Published on Web 01/21/2000

TABLE 1: Summary of the PO_3 Harmonic Frequencies (cm^{-1}), Intensities (km/mol), and Oxygen 16/18 Isotopic Ratios

mode	ω	inten	R(16/18)
	B3LYP/6-31+G*		
e′	142.3	7.8	1.0441
a_2''	410.1	57.2	1.0226
a_1'	994.4	0	1.0608
e′	1083.2	63.6	1.0389
	B3LYP/6-31+G(2df)		
e′	142.8	10.3	1.0443
a_2''	425.2	54.7	1.0226
a_1'	1015.6	0	1.0608
e′	1112.4	70.2	1.0388
	CCSD(T)/6-31G*		
e′	51.0	17.1	1.0432
a_2''	399.8	49.0	1.0226
a_1'	983.5	0	1.0608
e′	1055.9	131.7	1.0398

TABLE 2: Summary of the PO_3^- Harmonic Frequencies (cm^{-1}), Intensities (km/mol), and Oxygen 16/18 Isotopic Ratios

mode	ω	inten	R(16/18)
	B3LYP/6-31+G*		
e′	462.9	71.7	1.0514
a_2''	458.0	60.7	1.0226
a_1'	971.7	0	1.0608
e′	1239.3	644.6	1.0320
	B3LYP/6-31+G(2df)		
e′	474.0	64.9	1.0514
a_2''	477.2	55.3	1.0226
a_1'	996.0	0	1.0608
e′	1264.0	619.7	1.0317
	CCSD(T)/6-31G*		
e′	483.3	68.0	1.0516
a_2''	471.9	60.7	1.0226
a_1'	990.5	0	1.0608
e′	1286.6	448.5	1.0316
	CCSD(T)/6-31+G(2df)		
e′	487.1	68.1	1.0514
a_2''	490.5	56.0	1.0226
a_1'	1006.5	0	1.0608
e′	1282.3	596.0	1.0318

to photolysis using a medium-pressure mercury arc (Philips, H39KB, 175 W) lamp.

IV. Results and Discussion

We first consider the computational study of PO_3 and PO_3^-, which is summarized in Tables 1−3. We then describe the new experimental work; these results are summarized in Table 4. The additional calculations performed to support the experimental study are summarized in Tables 5−12.

The ground state of PO_3 is $^2A_2'$, which has D_{3h} symmetry. PO_3^- is a closed shell and also has D_{3h} symmetry. The two species have very similar bond lengths; for example, at the CCSD(T)/6-31+G(2df) level, the P−O bond length in PO_3^- is 1.492 Å compared with 1.482 Å for PO_3. At this level of theory, the electron affinity of PO_3 is 4.99 eV, which is similar to the value of 4.77 eV found at the B3LYP/6-31+G(2df) level.

The computed PO_3 and PO_3^- harmonic frequencies and intensities are summarized in Tables 1 and 2. Excluding the e′ bending mode of PO_3, all of the results are fairly independent of the level of theory used. The experimental bands at 480.3 and 1273.3 cm^{-1} with ^{16}O to ^{18}O isotopic ratios (R(16/18)) of 1.0219 and 1.0314, respectively, agree better with the computed results for PO_3^- than for PO_3. This is especially true for the 1273.3 cm^{-1} band, where the computed PO_3 value differs by more than 100 cm^{-1} with experiment, while the value for PO_3^- differs by much less. The experimental band at 435.2 cm^{-1} with an isotopic ratio of 1.0340 does not correspond very well with either PO_3 or PO_3^-.

TABLE 3: Summary of the Vertical Excitation Energies (eV) and f Values of PO_3 and PO_3^-

PO_3			PO_3^-		
state	Δ	f	state	Δ	f
$^2E''$	1.30	0.0000	$^1A_2'$	4.42	0.0000
$^2E'$	1.96	0.0014	$^1E''$	5.62	0.0000
$^2E'$	4.21	0.0040	$^1A_2''$	5.65	0.0000
$^2A_1''$	4.23	0.0000	$^1E'$	6.23	0.0128

The in-plane O 2p orbitals perpendicular to the P−O bonds form a_2' and e′ orbitals. The a_2' orbital is singly occupied in neutral PO_3, but doubly occupied in the anion. The one fewer electron should reduce the O−O repulsion in the neutral and may be responsible for the lower in-plane e′ bending frequency for PO_3 than for PO_3^-.

The electronic spectra of PO_3 and PO_3^- are computed using the time-dependent B3LYP approach using the 6-31+G(d) basis set at the PO_3 B3LYP/6-31+G(2df) geometry, and the results are summarized in Table 3. For PO_3^-, the first transition is at 4.42 eV, and the first allowed transition is at 6.23 eV. For PO_3, the computed transitions lie at 1.30, 1.96, 4.21, and 4.23 eV, with the transitions at 1.96 and 4.21 eV being allowed. The allowed transition at 1.96 eV agrees with the experimental value of 1.78 eV to within the expected uncertainty (±0.3 eV) of the theoretical method used. Since there are no other allowed transitions in this region, we agree with Withnall, McCluskey, and Andrews that the band they observe in experiment arises from PO_3 and should be assigned as $^2E' \leftarrow X^2A_2'$. The current results show that the progression at 525 cm^{-1} should be attributed to the upper state as done by Withnall, McCluskey, and Andrews. It is more difficult to assign the progression at about 900 cm^{-1}; the experimental value is similar to that of the a_1' mode of the PO_3 ground state, as suggested by Withnall, McCluskey, and Andrews, but the difference between theory and experiment is larger than expected. Given the size of the difference between theory and experiment for the vibrational frequency and the matrix temperature (12 K), we would be more tempted to assign this to the upper state than to the ground state.

While the assignment of the 480.3 and 1273.3 cm^{-1} bands to PO_3^- seems straightforward, it is disconcerting that the e′ bending mode of PO_3^-, which has about the same intensity as the a_2'' mode, cannot be assigned to any of the observed bands. Also, given that the electronic spectra clearly show the existence of PO_3, it is disconcerting that e′ P−O stretching and a_2'' out-of-plane bending modes of PO_3 have not been observed.

Early experiments employed laser-ablated red phosphorus as a reagent for dioxygen diluted in argon.[14] Similar experiments were done using lower oxygen concentration, lower laser power, and a rotating red phosphorus target to minimize the amount of ablated phosphorus and to favor the ablation of P atoms. Representative spectra are shown in Figures 1−3, and the absorptions are listed in Table 4; the related theoretical data are presented in Tables 5−12.

The strong sharp 1319.0 cm^{-1} absorption has been assigned to the antisymmetric stretching fundamental (ν_3) of PO_2 in solid argon.[1,14−18] This absorption is red-shifted 8.5 cm^{-1} from the gas-phase[19] diode laser value of 1327.53 cm^{-1}. The reaction with $^{18}O_2$ displaces the 1319.0 cm^{-1} absorption to 1280.0 cm^{-1}. The associated bending mode was observed at 386.8 cm^{-1} in other experiments using a grating instrument. Both infrared

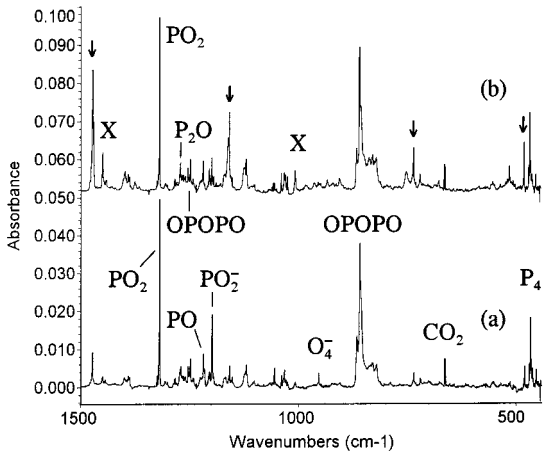

Figure 1. Infrared spectra in the 1500−445 cm^{-1} region for laser-ablated red phosphorus and 1% O_2 in argon: (a) sample codeposited at 10 K for 1 h and (b) sample after annealing to 25 K.

TABLE 4: Infrared Absorptions (cm^{-1}) from Codeposition of Laser-Ablated P with O_2 in Excess Argon

$^{16}O_2$	$^{18}O_2$	*R*(16/18)	assignment
1473.1	1431.1	1.0293	O_2PPO_2
1449.5	1407.7	1.0297	X($O_2P-O-PO$ isomer)
1319.0	1280.0	1.0304	PO_2
1270.3	1234.1	1.0293	P_2O
1253.4	1207.5	1.0380	OPOPO
1247.8	1203.9	1.0365	OPOPO
1218.0	1172.8	1.0385	PO
1198.6	1160.6	1.0327	PO_2^-
1158.1	1105.5	1.0476	O_2PPO_2
1007.5	971.7	1.0368	X($O_2P-O-PO$ isomer)
859.3	822.9	1.0442	OPOPO
735.1	703.0	1.0457	?
513.6	503.3	1.0205	?
480.2	469.9	1.0219	PO_3^-
479.4	459.1	1.0442	O_2PPO_2
465.8	465.8		P_4

active modes of PO_2 are in satisfactory agreement with our B3LYP calculations; compare the results in Tables 4 and 5.

The next strongest absorption at 1198.6 cm^{-1} has been assigned to the PO_2^- anion;[14,16] the $^{18}O_2$ counterpart appears at 1160.6 cm^{-1}. Our yield is not sufficient to observe the bending mode reported at 470 cm^{-1} in the gas phase.[20] New experiments were performed to investigate the effect of a CCl_4 electron trap[21−24] on the relative yields of PO_2 and PO_2^-. Figure 2 shows that CCl_4 doping reduces the absorptions of PO_2 to 50%, of PO_2^- to 40%, of $P^{18}O_2^-$ to 57%, and of $P^{18}O_2^-$ to 27% of their values without CCl_4. (Part of the overall reduction may be due to a lower yield of P atoms as P_4 was reduced to 65% in the 0.2% CCl_4 doped 1% O_2 experiment; this probably arises from ablation out of the groove on the target used in the previous experiment.) Annealing to 25 K reduced PO_2 by 20% and the PO_2^- band by 50%. Annealing to 30−40 K further decreased PO_2 and markedly increased O_2PPO_2 absorptions (Table 4). In addition, weak CCl_3 radical, CCl_3^+ cation, and $Cl-CCl_3$ transient absorptions were observed.[25−28]

The effect of added CCl_4 is to compete with PO_2 for ablated electrons and reduce the yield of anions relative to neutral molecules. In transition metal carbonyl systems, doping with 10% as much CCl_4 as CO present essentially eliminates the transition metal carbonyl anions from the spectrum. However, with NO and NO_2, CCl_4 doping reduced NO_2^- to 50% and $(NO)_2^-$ bands to 30% of the yields without CCl_4 added.[29] Clearly, NO_2 and PO_2 are good electron traps themselves, and

TABLE 5: B3LYP/6-31+G* Harmonic Frequencies (cm^{-1}), Intensities (km/mol), and ^{16}O to ^{18}O Isotopic Ratios for Species with One P Atom[a]

	^{16}O		^{18}O	
	ω	*I*	ω	*R*(16/18)
		PO		
σ	1226 (1218.0)	53	1181 (1172.8)	1.0380 (1.0385)
		PO_2		
a_1	381	31	376	1.0372
a_1	1047	4	995	1.0520
b_2	1277 (1319.0)	101	1238 (1280.0)	1.0312 (1.0304)
		PO_2^-		
a_1	445	38	427	1.0431
a_1	1031	84	986	1.0460
b_2	1172 (1198.6)	351	1135 (1160.6)	1.0331(1.0327)
		PO_3		
e′	142	8	136	1.0441
a_2''	410	57	401	1.0226
a_1'	994	0	937	1.0608
e′	1083	64	1042	1.0389
		PO_3^-		
e′	463	72	440	1.0514
a_2''	458 (480.2)	61	448 (469.9)	1.0226 (1.0219)
a_1'	973	0	916	1.0608
e′	1239	645	1201	1.0320

[a] The relevant experimental bands from Table 4 are given in parentheses for comparison.

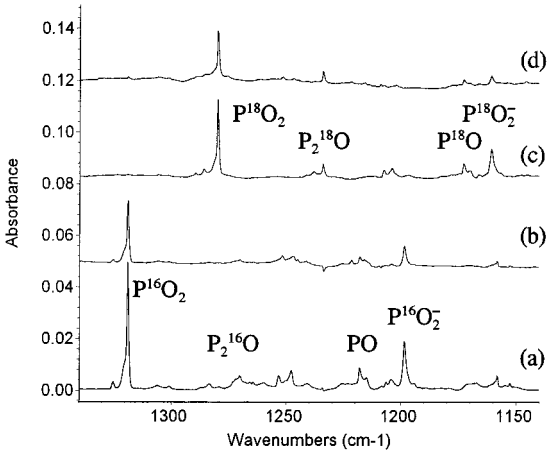

Figure 2. Infrared spectra in the 1340−1140 cm^{-1} region for laser-ablated red phosphorus and 1% O_2 in argon codeposited at 10 K for 1 h periods: (a) 1% O_2 in argon, (b) 1% O_2 and 0.2% CCl_4 in argon, (c) 1% $^{18}O_2$ in argon, and (d) 1% $^{18}O_2$ and 0.2% CCl_4 in argon.

they do not give in to CCl_4 as readily as transition metal carbonyls. Nevertheless, the decrease of PO_2^- absorptions relative to PO_2 bands is sufficient to confirm the PO_2^- anion assignment.

Figure 3 shows the lower region containing the PO_3^q, O_2PPO_2, and P_4 absorptions at 480.2, 479.4, and 465.8 cm^{-1}, respectively, in the 1% O_2 experiment.[1,15,16] The 480.2 cm^{-1} absorption was particularly noteworthy as it gave the 1/3/3/1 quartet with statistical $^{16,18}O_2$ characteristic of the nondegenerate motion of three equivalent oxygen atoms.[1] Doping with 0.2% CCl_4 reduced these band absorbances to 38%, 60%, and 65% of yields in the experiment without CCl_4. Annealing to 25 K slightly decreased the PO_3^q band, tripled the O_2PPO_2, band, and increased the P_4 absorption by 8%. The effect of added CCl_4 is to reduce the PO_3^q absorption at 480.2 cm^{-1} sufficiently to conclude that $q = -1$. Reassignment of the 480.2 cm^{-1} band to PO_3^- is indicated by the present calculations and experiments.

We do not observe any band that we can assign as the e′

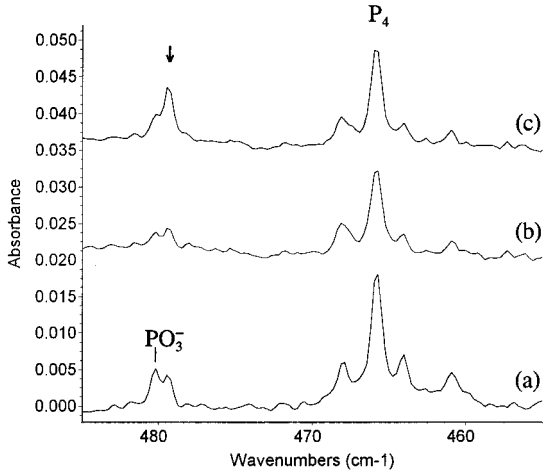

Figure 3. Infrared spectra in the 485−455 cm^{-1} region for laser-ablated red phosphorus and 1% O_2 in argon codeposited at 10 K for 1 h periods: (a) 1% O_2 in argon, (b) 1% O_2 and 0.2% CCl_4 in argon, and (c) after annealing to 25 K.

TABLE 6: B3LYP/6-31+G* Harmonic Frequencies (cm^{-1}), Intensities (km/mol), and ^{16}O to ^{18}O Isotopic Ratios for PPO and P_2O_2[a]

	^{16}O		^{18}O	
	ω	I	ω	R(16/18)
		PPO		
π	164	6	161	1.0168
σ	656	2	645	1.0166
σ	1266 (1270.3)	154	1228 (1234.1)	1.0310 (1.0293)
		P_2O_2		
b_{3u}	432	33	416	1.0389
b_{1u}	556	28	535	1.0389
a_g	606	0	601	1.0088
b_{3g}	700	0	671	1.0421
b_{2u}	725	104	697	1.0389
a_g	870	0	828	1.0515

[a] The relevant experimental bands from Table 4 are given in parentheses for comparison.

in-plane bending mode of PO_3^-, which is computed to be a strong transition and have a frequency very similar to that of the a_2'' band. The question naturally arises of whether the a_2'' and e′ bands are strongly overlapped. While the band at 480.2 cm^{-1} is definitely two overlapped bands, one grows on annealing and the other is the photosensitive band that we assign to PO_3^-. Given their different behaviors, it is difficult to assign these two components of the 480.2 cm^{-1} band to the same molecule. Thus, we see no evidence supporting the idea that the a_2'' and e′ bands are strongly overlapped.

The band at 1218.0 cm^{-1} is due to PO, and the B3LYP results are in good agreement; see Tables 4 and 5. The band at 1270.3 cm^{-1} with an isotopic ratio of 1.0293 is in very good agreement with the B3LYP results (1266 cm^{-1} and 1.0310) for the P−O stretch in the linear PPO species, which is also computed to have a large intensity; see Table 6.

We do not see any indication of P_2O_2 (planar with D_{2h} symmetry), which is computed to have a strong band at 724 cm^{-1}; see Table 6. However, the bands at 1253.4, 1247.8, and 859.3 cm^{-1} should be assigned, as previously suggested,[30] to the O═P−O−P═O isomer of P_2O_3, which is the most stable of the P_2O_3 isomers studied; compare the results in Tables 4 and 7. We do not see any evidence for the higher energy O_2-PPO isomer.

In previous P_2 oxidation experiments from this laboratory,[16,18] bands at 1438.4, 1168.1, and 955.4 cm^{-1} (labeled Y in the previous work) were assigned to oxo-bridged P_2O_4 (i.e., O_2P−O−PO). These bands are not observed in the present experiments, but the strongest calculated bands (Table 8) are compatible with this assignment. The earlier studies[16,18] also produced a species X (see Figure 1) absorbing at 1450.0 and 1007.9 cm^{-1}, which was attributed to structural isomers of oxo-bridged P_2O_4; these bands are observed here at 1449.5 and 1007.5 cm^{-1}, and they increase markedly on annealing (Figure 1).

TABLE 7: B3LYP/6-31+G* Harmonic Frequencies (cm^{-1}), Intensities (km/mol), and ^{16}O to ^{18}O Isotopic Ratios for P_2O_3[a]

	^{16}O		^{18}O	
	ω	I	ω	R(16/18)
		O═POP═O (E = 0.0 kcal/mol)		
a	61	1	58	1.0569
b	91	8	88	1.0391
a	102	4	98	1.0336
b	372	55	356	1.0441
a	452	22	428	1.0548
a	546	3	544	1.0046
b	823 (859.3)	1029	787 (822.9)	1.0461 (1.0442)
b	1248 (1247.8)	100	1201 (1203.9)	1.0392 (1.0365)
a	1264 (1253.4)	112	1218 (1207.5)	1.0385 (1.0380)
		PO_3P Tribridge (E = 24.1 kcal/mol)		
e″	355	0	342	1.0374
e′	512	67	489	1.0474
a_1'	700	0	687	1.0182
a_2''	726	354	703	1.0329
e′	750	229	717	1.0462
a_1'	860	0	826	1.0419
		O_2PPO (E = 34.2 kcal/mol)		
a	35	8	34	1.0384
a	100	2	95	1.0440
a	163	20	156 .	1.0437
a	239	46	233	1.0244
a	371	74	362	1.0246
a	485	7	473	1.0253
a	1101	82	1050	1.0489
a	1234	105	1188	1.0393
a	1371	169	1329	1.0314

[a] The relevant experimental bands from Table 4 are given in parentheses for comparison.

Sharp absorptions observed here at 1473.2, 1158.2, 735.1, and 479.4 cm^{-1} (labeled ↓) increased markedly (×4) on annealing to 25 K. These bands were assigned to P_2O_5 after formation in six different phosphorus/oxygen experiments.[1,14−18] The most important diagnostic evidence is the triplet of triplets first reported for the 1158.1 cm^{-1} band using statistical isotopic oxygen.[1] This clearly indicates two equivalent PO_2 groups each with equivalent oxygen atoms. Furthermore, the 1473.2 and 1158.1 cm^{-1} bands show 16/18 isotopic ratios for antisymmetric and symmetric P−O stretching modes in a phosphoryl subgroup. The current P_2O_5 B3LYP calculations (see Table 9) and the older HF/6-21G* calculations of Lohr[4] find a C_2 structure with inequivalent O atoms and a splitting in the strong antisymmetric O−P−O stretching mode. Furthermore, both calculations predict the strongest band, the antisymmetric P−O−P stretching mode, in the 900−1000 cm^{-1} region; no such band is observed in the spectrum. Therefore, the calculations cast doubt on the earlier P_2O_5 assignment.

The next best possibility is O_2PPO_2, the D_{2d} form of symmetrical P_2O_4. The strongest band (e) calculated at 1432 cm^{-1} with a 1.0309 16/18 ratio is appropriate for the antisymmetric PO_2 mode and the 1106 cm^{-1} band for the out-of-phase symmetric PO_2 mode. The computed 16/18 ratios are in good agreement with those determined experimentally. Scale factors

TABLE 8: B3LYP/6-31+G* Harmonic Frequencies (cm^{-1}), Intensities (km/mol), and ^{16}O to ^{18}O Isotopic Ratios for P_2O_4[a]

	^{16}O		^{18}O	
	ω	I	ω	R(16/18)
	O_2POPO Trans (E = 0.0 kcal/mol)			
a	28	1	27	1.0596
a	81	0	77	1.0535
a	118	6	114	1.0346
a	340	8	328	1.0365
a	382	119	367	1.0414
a	419	38	402	1.0427
a	481	16	462	1.0416
a	613	42	597	1.0256
a	868	635	826	1.0504
a	1139	175	1088	1.0465
a	1270	90	1222	1.0389
a	1429	175	1387	1.0304
	O_2POPO cis (E = 1.3 kcal/mol)			
a	29	11	28	1.0339
a	98	1	93	1.0538
a	108	6	103	1.0536
a	284	15	271	1.0473
a	359	39	348	1.0325
a	412	50	403	1.0240
a	461	67	442	1.0446
a	642	153	619	1.0371
a	882	516	839	1.0520
a	1143	239	1093	1.0451
a	1285	81	1237	1.0388
a	1423	177	1381	1.0304
	O_2PPO_2 D_{2d} (E = 24.5 kcal/mol)			
b_1	35	0	33	1.0608
e	143	26	136	1.0525
a_1	250	0	238	1.0495
e	343	42	337	1.0197
b_2	422 (479.4)	188	407 (459.1)	1.0370 (1.0442)
a_1	541	0	528	1.0230
b_2	1106 (1158.1)	147	1051 (1105.5)	1.0522 (1.0476)
a_1	1138	0	1085	1.0481
e	1432 (1473.1)	279	1389 (1431.1)	1.0309 (1.0293)

[a] The relevant experimental bands from Table 4 are given in parentheses for comparison.

that bring the B3LYP frequencies for these two modes into agreement with experiment, 1.029 and 1.047, are comparable. The computed band at 422 cm^{-1} is consistent with the experimental band at 479.4 cm^{-1}, but the differences bletween the B3LYP and experiment are slightly larger than for the other two bands. The O_2PPO_2 form of P_2O_4 is 24.5 kcal/mol above the O_2POPO form, but the formation process probably has more to do with the approach geometry of the reactants than with the relative energetics of the two isomers of P_2O_4. This reassignment requires that the 735.1 cm^{-1} band be due to another species, which grows on annealing in this reactive system. This absorption position and isotopic ratio are characteristic of the PO_3P tribridge (Table 7).

Finally, note the agreement between the B3LYP-calculated frequencies and the five strongest bands assigned to P_4O_{10} in solid argon[14] (1408, 1026, 767, 577, and 412 cm^{-1}). Again the calculated frequencies (see Table 10) must be scaled upward (in contrast to HF calculations) with scale factors 1.026, 1.050, 1.046, 1.053, and 1.051 for these infrared bands. The size of these scale factors is consistent with those found for O_2PPO_2.

Since bands associated with P_4 are clearly seen in these experiments, we have also considered P_3O and P_4O, which are possible products of the reaction of P_4 with oxygen. The results of these calculations are summarized in Tables 11 and 12. We have considered several structures for each system, but we have not found any definitive evidence of these species in the present experimental spectra.

TABLE 9: B3LYP/6-31+G* Harmonic Frequencies (cm^{-1}), Intensities (km/mol), and ^{16}O to ^{18}O Isotopic Ratios for P_2O_5

	^{16}O		^{18}O	
	ω	I	ω	R(16/18)
	O_2POPO_2 (E = 0 kcal/mol)			
a	56	0	53	1.0608
b	61	3	57	1.0659
a	103	1	98	1.0540
a	306	7	291	1.0529
b	336	13	323	1.0396
a	379	13	371	1.0235
b	421	69	407	1.0344
b	428	160	410	1.0431
a	487	2	467	1.0434
a	671	48	647	1.0364
b	938	490	889	1.0551
b	1129	317	1076	1.0493
a	1158	21	1105	1.0472
b	1445	136	1401	1.0313
a	1453	174	1409	1.0308
	O_2PO_2PO (E = 3.9 kcal/mol)			
b_2	88	5	84	1.0391
b_1	102	4	96	1.0604
a_2	245	0	231	1.0608
a_1	315	2	300	1.0495
b_1	323	5	314	1.0290
b_2	368	54	356	1.0333
b_1	447	51	429	1.0415
b_2	456	39	432	1.0542
a_1	512	299	501	1.0235
a_1	589	120	559	1.0534
a_1	970	40	915	1.0598
b_2	1082	148	1046	1.0350
a_1	1126	154	1072	1.0506
a_1	1418	220	1376	1.0304
b_1	1443	182	1402	1.0299
	OPO_3PO (E = 15.0 kcal/mol)			
e′	240	22	227	1.0578
e″	267	0	264	1.0131
e″	409	0	386	1.0602
e′	585	96	556	1.0507
a_1′	603	0	584	1.0329
a_2″	657	236	625	1.0509
e′	869	459	837	1.0381
a_1′	880	0	830	1.0607
a_2″	1358	442	1312	1.0349
a_1′	1438	0	1401	1.0271

TABLE 10: B3LYP/6-31+G* Harmonic Frequencies (cm^{-1}), Intensities (km/mol), and ^{16}O to ^{18}O Isotopic Ratios for P_4O_{10}[a]

	^{16}O		^{18}O	
	ω	I	ω	R(16/18)
e	238	0	225	1.0556
t_1	251	0	241	1.0393
t_2	257	51	247	1.0387
e	320	0	307	1.0422
t_1	387	0	381	1.0165
t_2	392 (412)	77	383	1.0248
a_1	523	0	508	1.0303
t_2	548 (577)	28	530	1.0347
a_1	684	0	646	1.0590
t_2	733 (767)	432	716	1.0238
t_1	794	0	767	1.0342
e	798	0	780	1.0229
t_2	979 (1026)	2099	949	1.0309
t_2	1378 (1408)	1176	1347	1.0223
a_1	1409	0	1366	1.0313

[a] The experimental values (McCluskey and Andrews[14]) are given in parentheses for comparison.

TABLE 11: B3LYP/6-31+G* Harmonic Frequencies (cm^{-1}), Intensities (km/mol), and ^{16}O to ^{18}O Isotopic Ratios for Species with Three P Atoms

	^{16}O		^{18}O	
	ω	I	ω	R(16/18)
	P_3O Rhombus (E = 0.0 kcal/mol)			
b_1	162	0	157	1.0307
b_2	368	13	368	1.0000
a_1	409	3	405	1.0109
a_1	533	6	533	1.0003
b_2	641	18	615	1.0413
a_1	730	67	792	1.0395
	O=PP_2 (E = 13.1 kcal/mol)			
b_1	208	9	204	1.0189
b_2	257	12	249	1.0294
a_1	328	3	327	1.0045
b_2	490	4	490	1.0010
a_1	555	11	548	1.0125
a_1	1254	171	1213	1.0336

TABLE 12: B3LYP/6-31+G* Harmonic Frequencies (cm^{-1}), Intensities (km/mol), and ^{16}O to ^{18}O Isotopic Ratios for Species with Four P Atoms and Zero or One Oxygen[a]

	^{16}O		^{18}O	
	ω	I	ω	R(16/18)
	P_4			
e	365	0		
t_2	461 (465.8)	5		
a_1	604	0		
	P_4O (Ring) (E = 0.0 kcal/mol)			
a_2	207	0	207	1.0000
b_1	297	6	286	1.0394
b_2	313	2	312	1.0007
a_1	426	5	418	1.0183
a_1	458	14	454	1.0074
a_1	521	5	521	1.0002
b_2	550	9	550	1.0001
a_1	620	39	604	1.0266
b_2	768	25	734	1.0462
	P_4O (Edge) (E = 12.7 kcal/mol)			
b_1	315	6	303	1.0386
a_1	327	0	325	1.0053
a_2	336	0	336	1.0000
b_1	412	5	411	1.0001
a_1	421	1	418	1.0073
b_2	441	9	441	1.0002
a_1	537	6	537	1.0007
b_2	637	35	612	1.0400
a_1	717	68	690	1.0394
	O=PP_3 (E = 29.0 kcal/mol)			
e	228	26	222	1.0291
e	323	0	323	1.0000
a_1	397	0	393	1.0110
e	496	18	496	1.0008
a_1	548	0	543	1.0085
a_1	1221	183	1182	1.0330

[a] The relevant experimental bands from Table 4 are given in parentheses for comparison.

V. Conclusions

The computed frequencies and experiment suggest that the band at 480.3 cm^{-1} should be reassigned to PO_3^-. The computed results show that the related band at 1273.3 cm^{-1} also agrees much better with PO_3^- than PO_3. This reassignment is a clear example of the synergistic effect of applying both theory and experiment to the identification of IR bands.

The computed results also suggest that the observed electronic transition is correctly assigned as the $^2E' \leftarrow X^2A_2'$ band system of PO_3. The new experimental work does not show any infrared evidence for PO_3, but we are able to identify bands associated with PO_2, PO_2^-, P_2O, OPOPO, and O_2PPO_2. P_4 is also observed in experiment, but we are unable to observe any evidence for the expected products such as P_4O and P_3O.

Acknowledgment. L.A. thanks the National Science Foundation (Grant CHE 97-00116) for financial support.

References and Notes

(1) Withnall, R.; Andrews, L. *J. Phys. Chem.* **1988**, *92*, *4610.*
(2) Withnall, R.; McCluskey, M.; Andrews, L. *J. Phys. Chem.* **1989**, *93*, 126.
(3) Bauschlicher, C. W. *J. Phys. Chem. A* **1999**, *103*, 11126.
(4) Lohr, L. L. *J. Phys. Chem.* **1984**, *88*, 5569. Lohr, L. L; Boehm, R. C. *J. Phys. Chem.* **1987**, *91*, 3203. Lohr, L. L. *J. Phys. Chem.* **1990**, *94*, 1807. Lohr, L. L. *J. Phys. Chem.* **1992**, *96*, 119.
(5) Becke, A. D. *J. Chem. Phys.* **1993**, *98*, 5648.
(6) Stephens, P. J.; Devlin, F. J.; Chabalowski, C. F.; Frisch, M. J. *J. Phys. Chem.* **1994**, *98*, 11623.
(7) Frisch, M. J.; Pople, J. A.; Binkley, J. S., *J. Chem. Phys.* **1984**, *80*, 3265 and references therein.
(8) Stratmann, R. E.; Scuseria, G. E.; Frisch, M. J. *J. Chem. Phys.* **1998**, *109*, 8218.
(9) Bartlett, R. J. *Annu. Rev. Phys. Chem.* **1981**, *32*, 359.
(10) Raghavachari, K.; Trucks, G. W.; Pople, J. A.; Head-Gordon, M. *Chem. Phys. Lett.* **1989**, *157*, 479.
(11) Gaussian 98, Revision A.6: M. J. Frisch, G. W. Trucks, H. B. Schlegel, G. E. Scuseria, M. A. Robb, J. R. Cheeseman, V. G. Zakrzewski, J. A. Montgomery, Jr., R. E. Stratmann, J. C. Burant, S. Dapprich, J. M. Millam, A. D. Daniels, K. N. Kudin, M. C. Strain, O. Farkas, J. Tomasi, V. Barone, M. Cossi, R. Cammi, B. Mennucci, C. Pomelli, C. Adamo, S. Clifford, J. Ochterski, G. A. Petersson, P. Y. Ayala, Q. Cui, K. Morokuma, D. K. Malick, A. D. Rabuck, K. Raghavachari, J. B. Foresman, J. Cioslowski, J. V. Ortiz, B. B. Stefanov, G. Liu, A. Liashenko, P. Piskorz, I. Komaromi, R. Gomperts, R. L. Martin, D. J. Fox, T. Keith, M. A. Al-Laham, C. Y. Peng, A. Nanayakkara, C. Gonzalez, M. Challacombe, P. M. W. Gill, B. Johnson, W. Chen, M. W. Wong, J. L. Andres, C. Gonzalez, M. Head-Gordon, E. S. Replogle, and J. A. Pople, Gaussian, Inc., Pittsburgh, PA, 1998.
(12) ACES II is a computational chemistry package especially designed for coupled cluster and many body perturbation calculations. The SCF, transformation, correlation energy, and gradient codes were written by J. F. Stanton, J. Gauss, J. D. Watts, W. J. Lauderdale, and R. J. Bartlett. The two-electron integrals are taken from the vectorized MOLECULE code of J. Almlöf and P. R. Taylor. ACES II includes a modified version of the ABACUS integral derivatives program, written by T. Helgaker, H. J. Jensen, P. Jørensen, J. Olsen, and P. R. Taylor, and the geometry optimization and vibrational analysis package written by J. F. Stanton and D. E. Bernholdt.
(13) Burkholder, T. R.; Andrews, L. *J. Chem. Phys.* **1991**, *95*, 8697.
(14) McCluskey, M.; Andrews, L. *J. Phys. Chem.* **1991**, *95*, 3545.
(15) Andrews, L.; Withnall, R. *J. Am. Chem. Soc.* **1988**, *110*, 5606.
(16) Andrews, L.; McCluskey, M.; Mielke, Z.; Withnall, R. *J. Mol. Struct.* **1990**, *222*, 95.
(17) Mielke, Z.; McCluskey, M.; Andrews, L. *Chem. Phys. Lett.* **1990**, *165*, 146.
(18) McCluskey, M.; Andrews, *L. J. Phys. Chem.* **1991**, *95*, 2988.
(19) Qian, H.-B.; Davis, P. B.; Hamilton, P. *A. J. Chem. Soc., Faraday Trans.* **1995**, *91*, 2993.
(20) Xu, C.; de Beer, E.; Neumark, D. M. *J. Chem. Phys.* **1996**, *104*, 2749.
(21) Illenberger, *E. Ber. Bunsen-Ges. Phys. Chem.* **1982**, *86*, 252; Matejcik, S.; Kiendler, A.; Stamatovic, A.; Mark, T. D. *Int. J. Mass. Spectrom. Ion Processes.* **1995**, *149/150*, 311.
(22) Zhou, M. F.; Andrews, L. *J. Am. Chem. Soc.* **1998**, *120*, 11499.
(23) Zhou, M. F.; Chertihin, G. V.; Andrews, L. *J. Chem. Phys.* **1998**, *109*, 10893.
(24) Zhou, M. F.; Andrews, L. *J. Phys. Chem. A* **1999**, *103*, 2964.
(25) Andrews, L. *J. Chem. Phys.* **1968**, *48*, 972.
(26) Jacox, M. E.; Milligan, D. E. *J. Chem. Phys.* **1971**, *54*, 3935.
(27) Prochaska, F. T.; Andrews, L. *J. Chem. Phys.* **1977**, *67*, 1091 and references therein.
(28) Maier, G.; Reisenauer, H. P.; Hu, J.; Hess, B. A., Jr.; Schaad, L. J. *Tetrahedron Lett.* **1989**, *30*, 4105.
(29) Zhou, M. F.; Andrews, L. *J. Chem. Phys.* **1999**, *111*, 6036.
(30) McCluskey, M.; Andrews, L. *J. Phys. Chem.* **1991**, *95*, 2679.